INVITED PAPER

Dynamic Surface Temperature Measurements in ICs

High-sensitivity, high-resolution thermal mapping of integrated circuits can be provided by techniques such as scanning with laser beams and embedding of CMOS temperature sensors.

By Josep Altet, Wilfrid Claeys, Stefan Dilhaire, and Antonio Rubio

ABSTRACT | Measuring techniques of the die surface temperature in integrated circuits are reported as very appropriate for failure analysis, for thermal characterization, and for testing modern devices. The paper is arranged as a survey of techniques oriented towards measuring the temperature dynamics of the circuit surface and presenting and discussing both the merits and drawbacks of each technique with regard to the accuracy, reliability and efficiency of the measurements. Two methods are presented in detail: laser probing methods, based on interferometry and thermoreflectance, and embedded CMOS circuit sensors. For these techniques, the physical principles, the state of the art in figures of merit and some application examples are presented.

KEYWORDS | CMOS temperature sensors; differential temperature sensors; integrated circuits (ICs); laser interferometry; laser thermoreflectance; temperature measurements

I. INTRODUCTION: NEW CHALLENGES FOR IC TEMPERATURE MEASUREMENTS

The temperature at the surface of an integrated circuit (IC) has a significant impact on the behavior, performance, and reliability of the semiconductor devices placed on it. Furthermore, temperature is a source of information regarding the state of all the elements involved in the heat transfer process throughout the IC structure. Consequently, having knowledge of the thermal map at the IC surface (the temperature distribution throughout the whole die surface) may enhance the design, modelling and observability of the devices, circuits and structure of an IC.

Within specialized literature, there is a considerable number of works where temperature analysis and measurements have been reported. From all such works, temperature sensing could be considered a mature topic. Nonetheless, scaling technology and design and test trends demand temperature measuring techniques with increasing performances. In each application area, due to its particular casuistry, temperature measurements face specific challenges.

For instance, in failure analysis, the detection and localization of hot spots is usually related to the localization of bridges and gate oxide shorts (GOS) [1]. Steady state temperature measurements with liquid crystal [2], infrared cameras [3], and fluorescent thermography [4] have been proposed and successfully used. Technology scaling directly affects these traditional methods in two senses: first, the increasing number of metal layers attenuates the temperature variations that can be measured at the IC surface [39]. Second, as devices become smaller, the lateral resolution of the temperature measuring systems has to be below 1 μm with sensitivities in the order of a few mK. In this direction, the use of dynamic temperature measurements has enhanced the capability of detecting hot spots in current technologies [35], [41], [57].

For the characterization of the thermal coupling in ICs, different measures are reported: static (dc) [7], transient in the time domain [6], or complex small-signal parameters (ac) in the frequency domain [8]. Nowadays, certain technologies demand spot temperature measurement (measuring temperatures in areas less than 1 μm^2), high lateral resolution (below 1 μm), small amplitude resolution (1 mK) and high bandwidth (compared to the bandwidth of the thermal coupling in the IC structure).

Traditionally, the thermal characterization of packages has been used for the characterization of their thermal resistance [9] and for the detection of defects in the

Manuscript received February 1, 2005; revised January 23, 2006.
J. Altet and **A. Rubio** are with the Department of Electronic Engineering, Technical University of Catalonia, Barcelona ES-08034, Spain (e-mail: pepaltet@eel.upc.edu; antonio.rubio@upc.edu).
W. Claeys and **S. Dilhaire** are with the Centre de Physique Moleculaire Optique et Hertzienne, Université Bordeaux I, Bordeaux F-33405, France (e-mail: w.claeys@cpmoh.u-bordeaux1.fr; s.dilhaire@cpmoh.u-bordeaux1.fr).
Digital Object Identifier: 10.1109/JPROC.2006.879793

package structure [13]. As technology evolves and power dissipation becomes the main design constraint, dynamic thermal models of packages (so-called thermal impedance) [10] are needed, requiring accurate, extended transient temperature measurements or low-frequency ac measurements [14] in different mounting configurations [11], [12], [15].

Temperature sensors embedded in an IC have been proposed in [44], [52], [58] to guarantee thermal integrity and safe values of the working temperature. In microprocessors, temperature sensors are being embedded in order to control the power dissipated by the circuit and thus ensure safe operating temperatures, e.g., by modulating the frequency of the clock signal [16]. In [17], ring oscillators are used to monitor the temperature in a field-programmable gate array (FPGA). Differential temperature sensors are used when the objective is to track the power dissipated by devices placed in the IC with independence of the ambient temperature [19]. For instance, in [53], transient differential thermal measurements taken with a built-in sensor are used to protect a current booster whereas, in [18], the transient activation of a hot spot is detected with this sensing strategy. In this case, the challenge is to design reliable temperature sensors compatible with the technology of the circuit whose temperature is observed.

In this paper, we will expose recent advances in temperature sensing strategies that offer interesting possibilities for current and future IC technologies: reflectometry, interferometry, and embedded temperature sensors. The common factors displayed by all these techniques are that they allow dynamic temperature measurements to be performed (beyond the full bandwidth of the thermal coupling mechanism in the IC structure), they offer interesting lateral resolutions, and they have sensitivities in the mK range.

The paper is organized as follows. Section II shows a survey of the temperature monitoring systems, classifying them and explaining their working principles and performances. Section III considers an electrical model of a typical measuring/monitoring system, in order to discuss the influence of different variables (ambient temperature, mounting configuration, IC structure) on the measured signal. Sections IV and V present a deep insight into two sensing categories: optical methods and embedded sensors. Finally, Section VI concludes the paper.

II. SURVEY OF TEMPERATURE MONITORING SYSTEMS

Temperature measurement methods can be divided into three categories [6], [59]: physically contacting methods, optical methods, and electrical or embedded methods.

In contact methods, either a device or a film is physically in contact with the surface of the IC and it is the temperature of this device or film that is actually measured. Typical devices are thermistors [62] or thermocouples [26], which are placed as a probe for a scanning thermal microscope (SThM, which, in fact, is an atomic force microscope). As an example, in [62], a platinum (Pt) wire is used as a temperature-dependent resistor. SThM measurements are very sensitive to surface roughness and the water layer on the surface as they affect the thermal exchange between the probe and the sample [60]. The lateral resolution under atmospheric pressure is about 100 nm, and it can reach 10 nm under vacuum.

Typical films are liquid crystals or fluorescent films. Liquid crystals are organic compounds whose visible color in the region being observed changes as the temperature of the region changes [2]. Fluorescent films are polymer films whose fluorescent quantum yield is heavily dependent on temperature [4].

The main drawback of contacting methods is that epoxy, metal, and passivation layers placed over the silicon die attenuate the temperature measured when compared to the real temperature at the silicon surface [26], [62].

Optical methods are based on measurements of light. Infrared thermography, reflectometry, and interferometry fall into this category. Infrared thermography measures the light emitted by the IC due to its absolute temperature. The phase and amplitude of the light reflected by the IC depend on the temperature. A reflectance laser probe measures variations in the amplitude of the reflected light, whereas an interferometer measures variations in the phase of the reflected light.

Layers placed over the silicon die, especially metal layers, may affect the performance of optical techniques. Temperature measurements can be done from backside or lateral measurements [21], [22]. Backside temperature measurement is invasive and need sample preparation. Thermoreflectance measurements have been done in [5] with 0.1 K resolution over fundamental electronic noise when using a 5-μm-diameter laser spot through a 200-μm substrate. Time gating thermoreflectance imaging seems to be a promising technique [61]. Comparable to optical coherence tomography, this technique allows 1-μm lateral resolution and 8-μm-depth tomographic resolution. The temperature sensitivity is about 1 mK.

Electrical or embedded methods are based on the temperature dependence of the electrical characteristics of an electronic device. The device can be stand-alone or part of a more complex circuit. The advantages of this technique are that it allows us to perform temperature measurements in the field application of the IC and does not require visual access to the silicon surface. However, the temperature measuring circuitry increases the semiconductor area (which is related to fabrication costs) and requires input/output pins to have access to the terminals of the sensor.

Table 1 gives figures of bandwidth, lateral resolution, and temperature resolution obtained through the different techniques as reported in the literature.

Table 1 Temperature Monitoring Methods Classification

CLASSIFICATION OF TEMPERATURE MONITORING METHODS	Bandwidth	Lateral resolution	Temperature resolution
NON EMBEDDED METHOD			
NON CONTACT METHODS			
Infrared emission thermography	50 kHz[23]	10 μm[1]	0.02°C[24]
Thermoreflectance	150 MHz	0.5 μm	0.001°C
Interferometry	150 MHz	0.5 μm	1 fm ~ 0.0001°C
CONTACT METHODS			
Liquid crystal thermography[25,67,68]	0.01 Hz	1 μm	0.1°C
Fluorescent microthermography[4]	0.01 Hz	0.7 μm	0.01°C
Scanning Thermal Microscopy[26]	100 kHz	50 nm	0.001°C
EMBEDDED METHODS			
Absolute temperature sensors	>1 MHz	No	
Differential temperature sensors[6]	>1 MHz	No	0.01 °C

The temperature measurements can be static or dynamic. Static temperature measurements are performed when devices dissipate a constant power, boundary conditions are time independent, and the thermal steady state is reached. In such circumstances, temperature does not depend on time. In dynamic measurements, the power dissipated by the devices tends to be time varying. These measurements can be categorized into two sets: transient, where the temperature is observed as a function of time, and ac (so-called small-signal or lock-in). In the latter group, the amplitude and phase of one spectral component of the temperature is observed. Such measurements are usually performed when the power dissipated by the devices can be expressed as a time periodical function.

AC measurements have the following advantages compared to transient measurements.

1) They are more robust to noise [57], [62], [63].
2) Amplitude and phase can be measured. Amplitude is usually affected by the calibration constant, whereas phase is not. Besides, phase measurements have been reported in some works to be more sensitive than amplitude. This makes phase temperature measurements an interesting source of information (e.g., [27], [39]–[41], [57], [62]).
3) As we shall see in the following section, by choosing the frequency of the spectral component of the temperature, the penetration depth of the heat in the IC can be controlled. Thus, the number of IC layers which may affect the temperature distribution at the silicon surface can be controlled [27], [39], [40].

III. MEASURING TEMPERATURE IN AN IC: GENERAL CONSIDERATIONS

The goal of this section is to present the key factors from which the IC structure, the characteristics of the dissipating device, and the placement/characteristics of the sensor impact on the dynamic of temperature measurements.

To establish a nomenclature, Fig. 1 shows a general representation of a measurement procedure. Let us suppose that devices or subcircuits in an IC dissipate power. Due to the thermal coupling in the IC structure, a nonhomogeneous thermal map at the silicon surface appears. With a sensor system, which in this section is assumed to be embedded in the IC, the temperature can be observed at one specific location of the silicon surface, causing a proportional electrical signal at the output of the sensor.

In the figure, a simplified equivalent electrical model of all the electrothermal mechanisms is drawn. It is simplified, as it is unidirectional and linear. The equivalence between electrical variables in the thermal part of the model and thermal variables in the IC is classical (e.g., [18]): temperature is modeled as voltage, and energy flow (i.e., heat flow or power) is modeled as current. The thermal coupling mechanism is modeled with the thermal coupling impedance in the IC Z_{th_c}, the thermal impedance

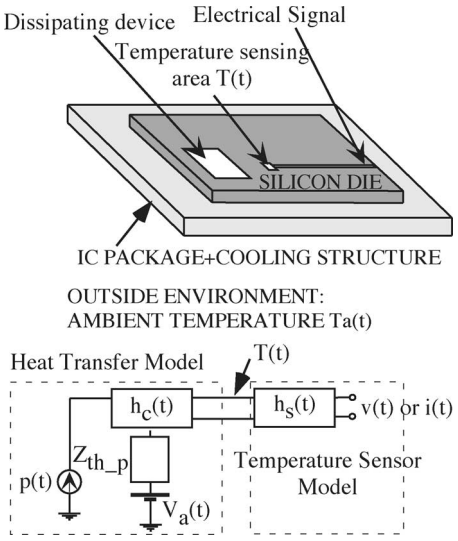

Fig. 1. *Electrical model of an IC temperature measurement procedure.*

from the package to the ambient Z_{th_p}, and the offset value generated by the ambient temperature $V_a(t)$. Finally, $h_s(t)$ models the transfer function of the sensor system, as its input is temperature and its output is an electrical signal [$v(t)$ or $i(t)$].

The model gives us an approach to the main contributors to the measured temperature $T(t)$ and allows us to analyze the effect of the different elements on the output voltage dynamics.

First, the dynamic characteristics of the thermal coupling exhibit a low pass filter behavior. The cutoff frequency is between 10 kHz and 1 MHz, depending on the distance between the dissipating device and the temperature measuring point/area. The lower limit of 10 kHz may be even lower if the temperature is not measured on the silicon surface. As an example, Fig. 2 shows two Bode diagrams of thermal coupling. The temperature is measured on the silicon surface with a differential temperature sensor (reported in Section V) and Bode diagrams are shown for two different distances between the dissipating device (an MOS transistor with an aspect ratio of 10 μm/1.2 μm) and the temperature observation area.

Second, the dynamic temperature measured on the surface reflects the thermal properties of the portion of the IC affected by the thermal transfer mechanism. As the thermal coupling mechanism is a diffusion process, the penetration depth in the IC structure of the heat injected by the dissipating elements depends on its spectral form.

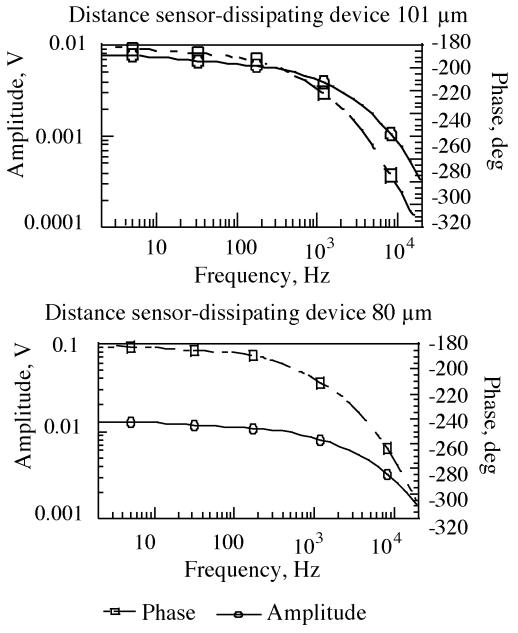

Fig. 2. *Measured Bode diagrams of the thermal coupling mechanism on the silicon surface for two different distances between the dissipating device and the temperature observation point: 80 and 101 μm. Silicon die: 3 mm × 2.5 mm. Package: ceramic DIL48.*

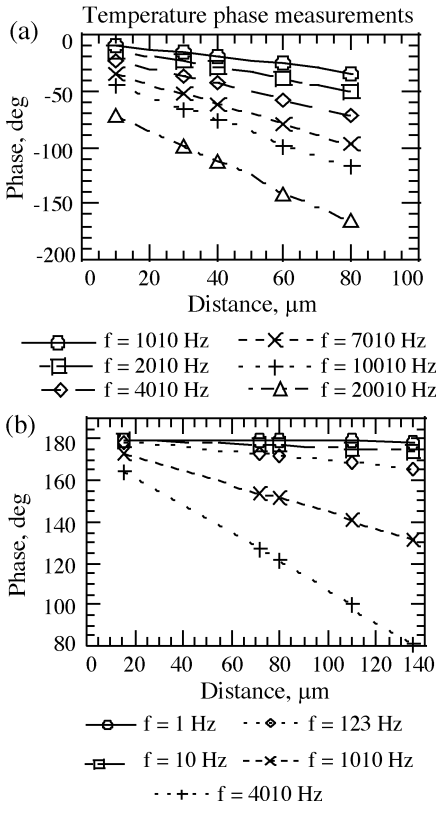

Fig. 3. *AC phase measurements for different frequencies as a function of the distance between the dissipating device and the temperature sensor. (a) Data obtained with a thermoreflectance laser probe. (b) Data obtained with an embedded differential temperature sensor.*

High-frequency components have a low penetration depth which increases as the frequency lowers.

To illustrate this, Fig. 3 shows ac phase temperature measurements (both power dissipation and temperature can be written as time dependent sinusoidal functions) performed with the differential temperature sensor described in Section V-B as well as with a thermoreflectance laser probe Section V-A. The vertical axis shows phase shift φ of the measured temperature as regards the periodic power dissipated by an MOS transistor (with an aspect ratio of 10 μm/1.2 μm), and the horizontal axis shows distance between the dissipating device and the temperature sensor. As we can see, all phase shifts are linear, with a slope that depends on the frequency.

Fig. 4 plots the value of this slope as a function of the frequency. In this function, two areas are highlighted. For high-frequency measurements, the function is a straight line of slope 1/2 when drawn on a log-log chart. This is due to the fact that for these frequencies the penetration depth of the injected energy is less than the dimensions of the die. The measured temperature behaves as if the material were a semi-infinite one [27]. The thermal impedance Z_{th_p} has no influence on the measured temperature.

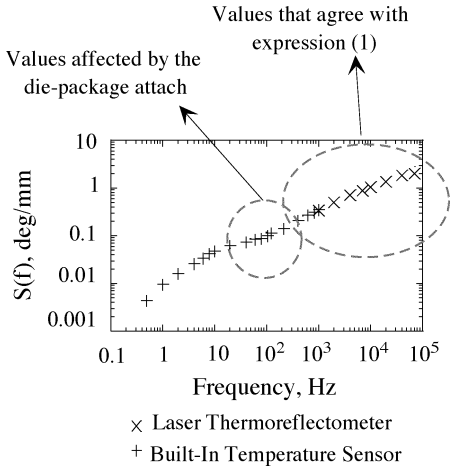

Fig. 4. ***Measurements of the function*** $S(f)$.

Measured data agrees with the analytical solution of a spherical dissipating device in an infinite material [64]

$$\varphi(r,f) = r\sqrt{\frac{\pi \cdot f}{D}}. \tag{1}$$

Where the phase shift (φ) depends on the physical properties of the silicon (thermal diffusivity D), frequency (f), and distance (r) between the measuring point and the dissipating device. Therefore, if the first two variables are known, the distance between the dissipating device and the measuring point can be obtained from phase measurements. As reported in the following section, temperature measurements performed within this frequency range can be applied for locating dissipating devices and so be used in failure analysis [39].

In the middle range of frequencies, the function $S(f)$ measured on the surface of the silicon depends on the thermal properties of the die attachment to the package [14].

As the frequency lowers, the penetration depth increases and the temperature on the surface depends on deeper elements of the IC structure, until Z_{th_p} is reached.

Similar reasoning and conclusions can be reached if the analysis and measurements are performed in the time domain: short activation of the dissipating devices has an associated low penetration depth. As the activation duration of the dissipating devices becomes larger, the penetration depth increases. As a matter of example, Fig. 5 depicts the structure of a metal line in an IC. Using a thermoreflectance laser probe, the transient temperature increases on the top of the metal are recorded when a current pulse passes through it. The same figure shows the absolute temperature transient response. On the nanosecond scale, the aluminum heat capacity plays the dominant role. Heat transfer through the SiO_2 becomes important on

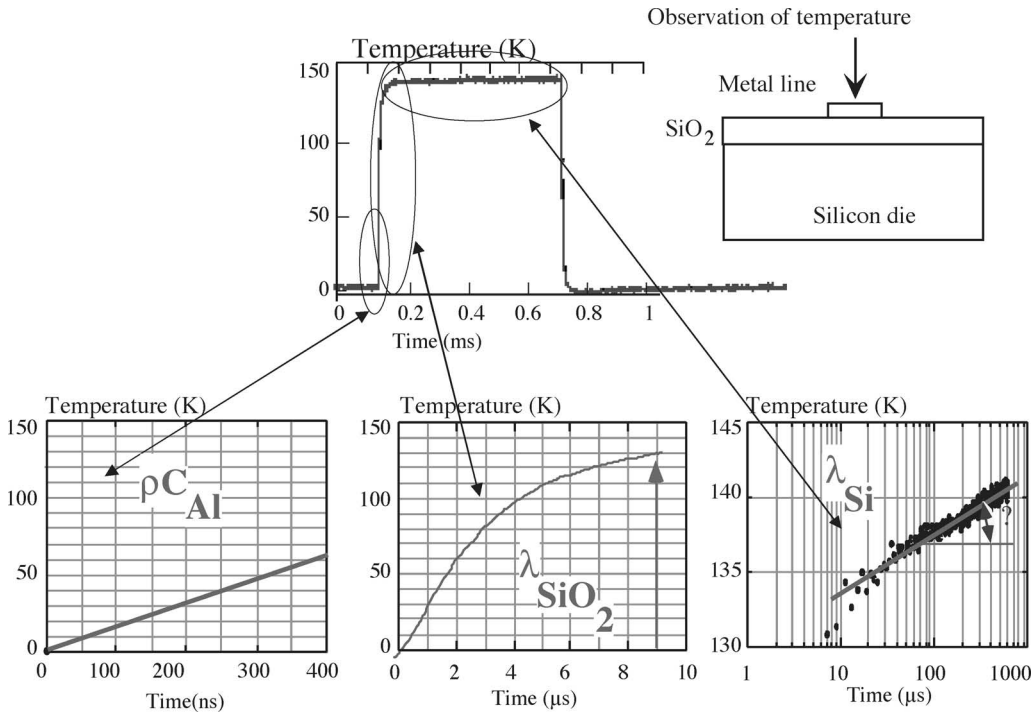

Fig. 5. ***Transient temperature of an aluminum line at different times after current is turned on. Layer thicknesses: aluminum: 0.5 μm. Silicon dioxide: 0.3–1 μm.***

the millisecond scale, while the thermal conductivity of the silicon die dominates the long time-domain response. From these measurements, it is possible to obtain the thermal properties of the different layers involved in the transport mechanism [28].

Going back to Fig. 1, ambient temperature affects all the measurements, as all the variables involved in the electrothermal process (power-dissipated, physical variables that influence thermal transfer, electrical variables of the sensor system, sensitivities) depend on it. Once it is set, then a "temperature operating point" is established and the value of all the physical and electrical parameters of all the blocks involved in the measurement can be known. Most of the measurement methods considered in this paper really measure temperature fluctuations over the reference temperature on the surface. When amplitude is measured, a calibration step is needed to obtain the exact value of the temperature change. On the other hand, when phase is measured, the effect of the reference temperature is negligible.

Finally, in Fig. 1, the block $h_s(t)$ models the dynamics of the sensor systems. When the sensor is embedded in the IC, $h_s(t)$ only models the electrical behavior of the sensor, as the temperature evolution of the sensor is included in the thermal coupling model. In other cases, especially in contact measuring methods, it is constituted by two blocks; the first one models the heat transfer from the IC to the sensor system, whereas the second models the electrical response of the sensor [29].

IV. OPTICAL TECHNIQUES

When an IC operates, it induces physical changes in the materials involved in its construction. Straightforward effects are, for example, variations of temperature that induces thermal expansion and corresponding deformation. By adopting appropriate methods, one can investigate different features of working electronic devices by analyzing optically the physics that take place in it [30]–[33]. In this section, we give an overview of the passive laser probing methods applied to electronic devices. By passive probing, we mean the laser has no measurable effect on the running device, it only "reads" the information. Two situations will be distinguished: the laser beam is highly focused in order to get a very small probing point or the laser lights up the entire device and imaging techniques are used to read the information contained in the reflected light.

We will limit this survey to methods where a laser beam is reflected back from the surface of the component under test (Fig. 6).

Somewhere, a device is running, producing time-dependent variations in the physical properties of the materials of the structure. Let us consider a surface point on such a device, where the laser reflection occurs. Even if the perturbation (heat generation by Joule effect, for example) is located inside the device the laser reading can be taken elsewhere.

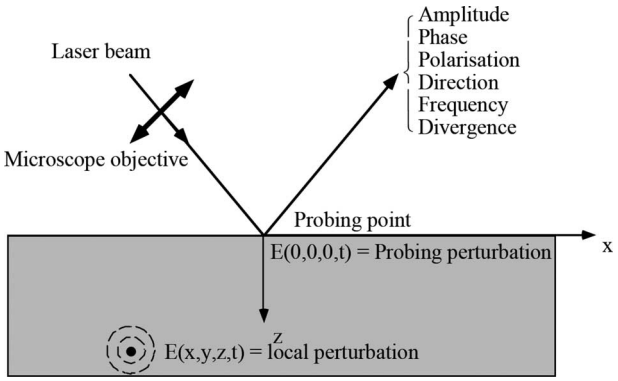

Fig. 6. *Sketch of probing principle.*

The outgoing laser light carries information of many different forms, such as the amplitude, phase, polarization, frequency, etc., as they can be influenced by the time-dependent physical property changes of the materials under the laser spot.

We will focus on amplitude (thermoreflectance) and phase measurements (interferometry) [34], [35]. The amplitude-phase description of the component reflectance can be expressed

$$\Re = R(t)e^{j\varphi(t)}$$

where $R(t)$ is the amplitude and $\varphi(t)$ the phase.

By performing separate amplitude and phase measurements, one is able to obtain information on different physical phenomena induced by the running of the device. Reflectance $R(t)$ is dependent on the temperature. Phase $\varphi(t)$ is dependent on the optical path length and, therefore, on surface displacement. The latter can be induced by the thermal expansion associated with internal temperature changes, by sound waves, or by thermoelastic waves in the running device.

Two development aspects are shown below:

- instrumentation for high-resolution amplitude and phase measurement;
- methods depending on the heat generation process, the localization of these processes, and their propagation to the measurement point.

A. Interferometry

One laser probe is a high resolution Michelson interferometer [35]; see Fig. 7. The laser is a stabilized, polarized HeNe laser ($\lambda = 632.8$ nm). The beam-splitting element of the interferometer is a polarizing prism. By rotating a half-wave plate ($\lambda/2$) in the incoming laser beam, it is possible to partition the intensity of the reference arm to that of the

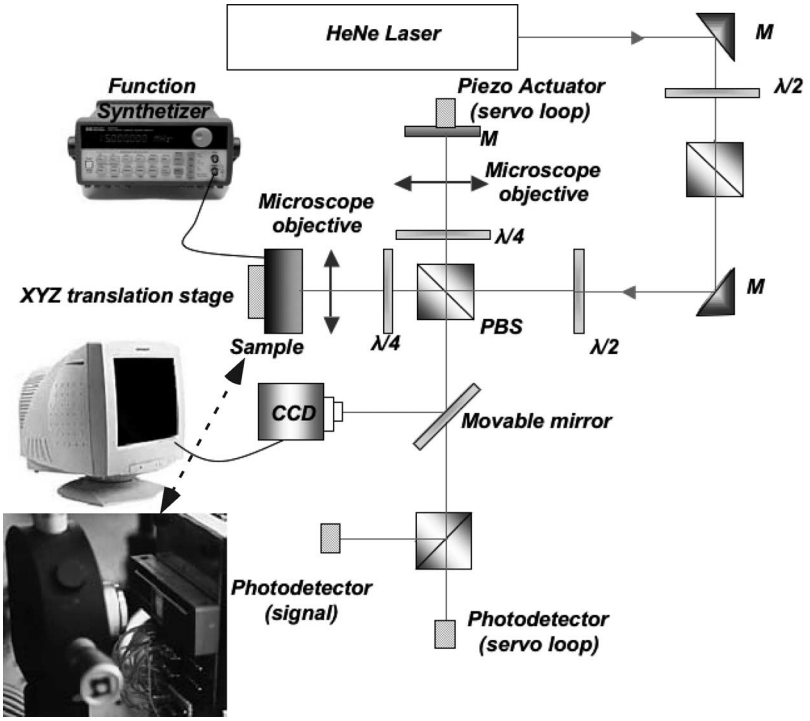

Fig. 7. *Schematic view of laser probe.*

probe arm so as to equalize the reflected intensities and obtain high-contrast interference fringes. In the reference and probe arm, a quarter-wave plate $(\lambda/4)$ is inserted. The linear polarization of the incoming light is rotated by 90° when coming out as it has passed the quarter-wave plate twice. This allows all the intensity of the returning beams to be reflected onto the photodetector while the polarizing prism acts as an optical insulator. The two beams have orthogonal linear polarizations. To obtain interferences, both polarizations are projected at 45° upon a single axis by passing through a polarized beam splitter before passing through the photodetector.

A microscope objective focuses the probe beam upon the surface of the component under test. The phase of the reflected beam is modulated by the normal surface displacements. The sample is mounted on a three-dimensional micrometric translation stage. The laser impact upon the sample can be viewed on a CCD camera by moving the mirror in front of the reflected probe beam and reducing the laser beam intensity with the attenuation placed in the laser beam. The lateral resolution is better than 1 μm. The interferometer is actively stabilized at the point of highest sensitivity (mid-fringe).

The detected signal is averaged in synchronism with the excitation signal and recorded by a digital oscilloscope or by a lock-in amplifier for small ac signal measurements.

The absolute values of the surface displacement are obtained from the comparison of the photodetected signal amplitude with the fringe signal amplitude from large displacements produced by moving the piezomirror in the reference arm.

The equipment allows us to measure the surface temperature locally through the dynamic deformation of the IC surface. The experimental sensitivity of the bench is obtained by measuring the normal surface displacement due to the Joule effect heating of a resistive layer upon an IC as a function of the electrical current amplitude going through it. The results are shown in Fig. 8. The amplitude of the displacement is plotted on a logarithmic scale. A slope of two is the signature of the quadratic dependency of the normal surface displacement amplitude versus current. The signal is detected down to amplitudes as small as a fraction of a femtometer (10^{-15} m), which is the shot noise detector limit.

B. Thermoreflectance

Thermoreflectance is the variation of the reflection coefficient of a material with temperature [33], [36]

$$R(T) = R_0 + \Delta R(T) = R_0(1 + \kappa \Delta T). \qquad (2)$$

If we focus a laser beam of intensity Φ_0 onto the material and detect with a photodiode the reflected light

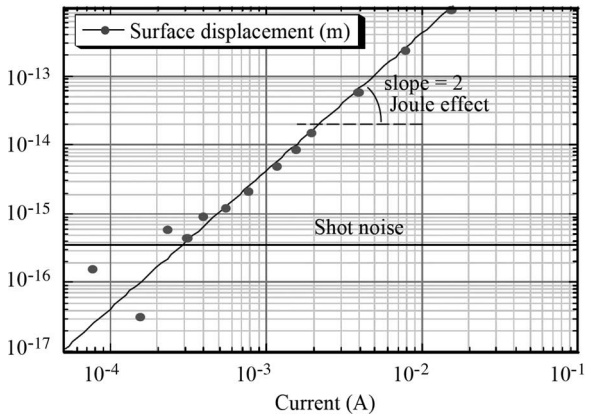

Fig. 8. ***Experimental sensitivity of the interferometer.***

intensity $R\Phi_0$, variations of the current I generated can be related to variations in the temperature $T(\Delta T)$ of the area targeted by the laser

$$\Delta T = \left(\frac{1}{R}\frac{\partial R}{\partial T}\right)^{-1}\frac{\Delta I}{I} = \kappa\frac{\Delta I}{I}. \qquad (3)$$

We see that with a simple optical probe, it is possible to measure dynamic temperature changes of normally working ICs. Absolute values can be readily obtained if $\kappa = (1/R)(\partial R/\partial T)$, the relative reflectance temperature coefficient, is known. For pure silicon, the value of $\kappa = 1.5 \cdot 10^{-4}$ is given by literature [37] and we found by a specific calibration procedure $1.35 \cdot 10^{-4}$ and $2.5 \cdot 10^{-5}$ for Al [38]. The experimental setup is the same as the one described in Fig. 7 with the difference that no light is sent to the reference arm. No interferences occur and the detector measures amplitude changes of the reflected laser beam. Experimentation shows the device to be a simple and excellent tool for IC surface temperature variation measurements. The optical probe is capable of measuring surface temperature changes in the range 10^{-3}–10^{2} K at a micrometric scale upon ICs. High resolution temperature mapping is possible and dynamic responses can be studied in the dc—125-MHz range with our photodetection system. The upper limit of 125 MHz is due to the bandwidth of the present electronic circuitry that reads the current generated by the photodiode.

C. Application Examples

One application for laser optical methods is temperature measurement: Fig. 9 shows the result obtained by scanning a laser beam across an IC where some components are running. The left-hand side of the figure shows the reflectance results with a 3-μm step, two aluminum metal lines; A and B can clearly be seen. The right-hand side shows the relative reflectance change between on and off. It can clearly be seen that only line A is functioning. By an appropriate calibration procedure, the relative reflectance change can be converted into absolute temperature changes. The method allows very small temperature changes to be determined as the scale covers a range from 0° to 6°.

Fig. 10 is the result of a scan with a 1-μm step. It shows the localization of hot spots at a micrometric scale. The temperature inhomogeneity is due to hillocks and voids arising from electromigration in the metal line.

Through measurements of the normal surface displacement, it is possible to detect and locate devices acting as hot spots, which is of interest in the field of test and failure analysis of ICs.

Both transient and small-signal ac interferometric measurements allow detection and localization of hot

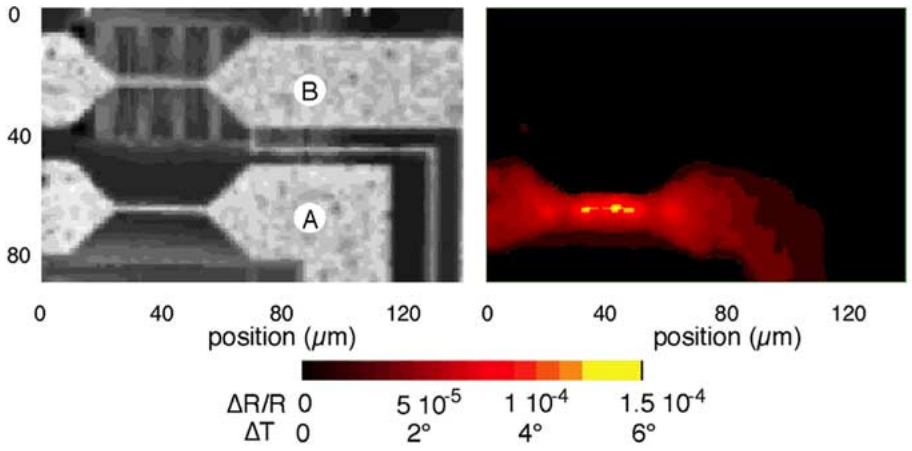

Fig. 9. ***Temperature mapping upon an IC.***

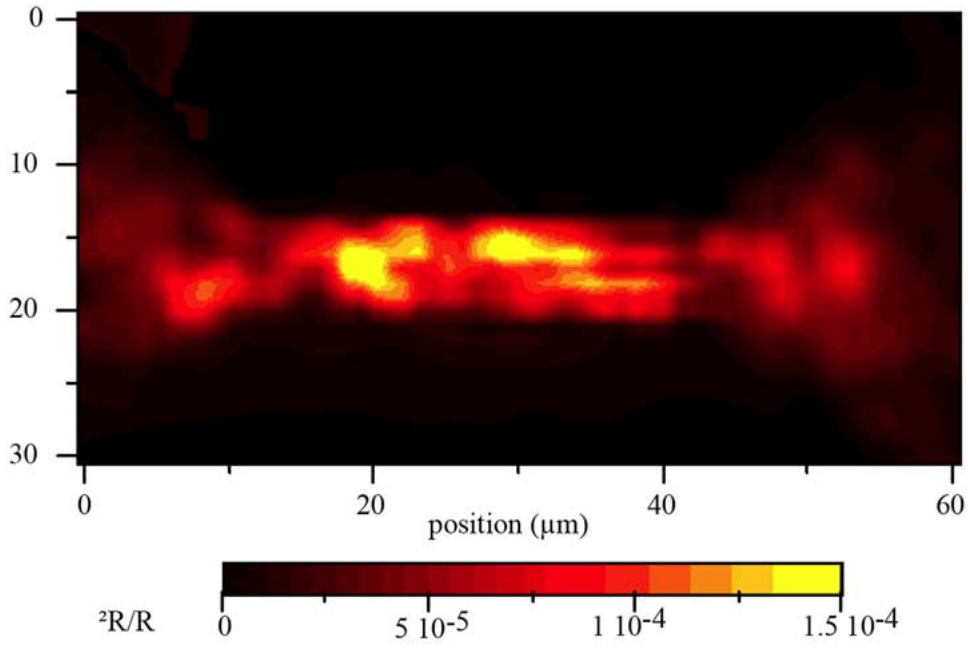

Fig. 10. ***Temperature mapping of metal line with micrometric lateral resolution.***

spots [39], [40]. Here we will focus on ac measurements, as they are more robust to noise. For the particular case of sine wave excitation, the power dissipation of such a hot spot has a periodic time dependency. The propagation of the heat flux in the IC produces an oscillating temperature field. As a consequence, an oscillating surface displacement at the same frequency at each point on the surface in the vicinity of the fault is produced. This field is called thermoelastic surface wave. The thermal properties of the material determine the amplitude and the phase of the temperature variation for a given frequency at a given location on the surface of the component.

Therefore, the surface of the chip has, at a given location, a displacement normal to the surface at the same frequency as the heat source. The amplitude and the phase of this surface movement depend upon the temperature distribution under the surface and the stress buildup in the medium. A detailed characterization of this phenomenon can be found in [36].

Fig. 11 shows a photo of an IC developed to test the capabilities for detecting and locating hot spots with the interferometer and reflectometer. The image shows eight MOS transistors that may dissipate power. In the experiment, the power dissipation of each transistor is individually controllable, allowing for a simple or multiple hot spot activation.

The use of a lock-in amplifier allows us to measure the phase of the response with respect to the sine wave current supplied to the active MOS transistor. For this IC, we observed that the phase behavior of the thermoelastic surface waves is the same as that described in Section III for the periodic thermal field (Fig. 3): for high-frequency activations, the phase shift of the wave at a certain distance from the MOS transistor only depends on the physical properties of the IC and the frequency of activation. Therefore, thermal waves emitted by the running transistors are used to localize the heat source by a phase shift measurement at three given points (P_1, P_2, and P_3) as shown in Fig. 11. The laser probe acts as an isotropic thermal antenna. From the phase shift measured in P_1 it is possible to determine the distance to the source D_1. We draw an initial circle or radius D_1 around P_1. In order to determine the position of the heat source, the measurement must

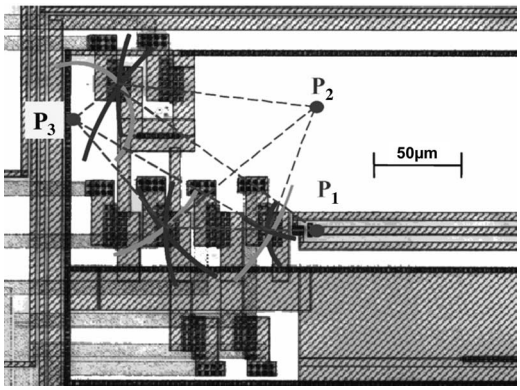

Fig. 11. ***Localization of heat sources by a set of three-phase shift measurements at*** P_1, P_2, ***and*** P_3.

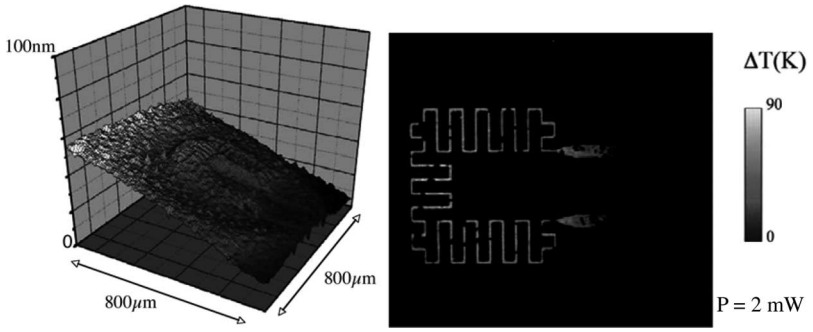

Fig. 12. ***Normal surface displacement of a membrane and temperature surface variation.***

be taken at three points (P_1, P_2, and P_3); the source is at the intersection of the three circles as shown in Fig. 11. Three heat sources #1, #3, and #5 have successively been activated and localized.

An interferometer was used in [41], [42] to detect and locate a hot spot in a 0.18-μm CMOS IC with five levels of metal and metal fills. In this case, due to the metal fills, no direct visual access to the silicon surface was possible. The metal fills were formed by electrically isolated rectangular metals. The laser probe allowed us to dynamically monitor the displacement of a single rectangle due to the heat dissipated by the device acting as a hot spot. These works show how it is possible to use amplitude and ac small-signal phase measurements to detect and locate the heat source. In the particular example of [42], if the hot spot produces dissipation higher than 890 μW, it can be detected and located through surface displacement measurements. For the case of amplitude measurements, the hot spot was beneath the metal fill whose displacement was maximal.

So far, we have considered the case of punctual measurement. Interferometric and thermoreflectance imaging (direct two-dimension image extraction) is possible based on classical electronic speckle pattern interferometry ESPI. In this case, the light source, usually a laser diode or an He–Ne laser, can be replaced by a light-emitting diode (LED). The laser lights up a complete area of the IC and the reflected light is collected by a CCD camera. Details about the instrumentation setup and information process of the technique can be found in [43]. As an example of measurement, Fig. 12 shows the normal surface displacement of a membrane and its temperature surface variation in a micromachined IC holding a metal line acting as a resistance.

V. EMBEDDED TEMPERATURE SENSORS

Embedded temperature sensors allow continuous dynamic and static monitoring of the surface temperature of the IC at specific locations. With this technique, temperature can be measured without having direct visual access to the silicon surface and measurements can be performed either in-field, even online, or in a test laboratory.

There are two major drawbacks to embedding temperature sensors: first, there is a silicon area overhead. Second, temperature can only be sensed in specific areas of the IC: the location of the temperature-sensitive devices which act as temperature transducers.

A specific requirement of the embedded temperature sensors is that they must be fully compatible with the technology process of the circuit into which they will be embedded [44]. The output signal of the temperature sensors can be proportional either to absolute temperature at one point of the silicon surface (Fig. 1) or to the difference in temperature at two points of the silicon surface (Fig. 13). This leads to the categorization of temperature sensors into two groups: absolute and differential.

A. Absolute Temperature Sensors

Absolute temperature sensors are used in today's high-performance microprocessors [16] in order to guarantee thermal integrity and safe operating temperatures in the IC. Other uses of embedded temperature sensors include the characterization of thermal impedances [8], [11] and the thermal testing of packages [13], [14]. Absolute temperature sensors may be categorized into single-device sensors or multiple-device sensors.

Single-device sensors are formed by a temperature sensitive device, whose sensitive terminals are accessible through the IC pins. Although all devices in an IC are temperature sensitive, the usual device for a single-device sensor is a PN junction (or a forward-biased bipolar transistor), due to its predictability, long-term stability, and linearity [45].

In the case of bipolar transistors, the key temperature-dependent parameter observed is its base-emitter voltage, whose sensitivity to temperature is almost linear with a typical value of -2 mV/K.

In the case of CMOS processes, vertical and lateral parasitic bipolar transistors may be used. In [45] and [46], vertical transistors are preferred as their electrical characteristics are closer to real bipolar transistors.

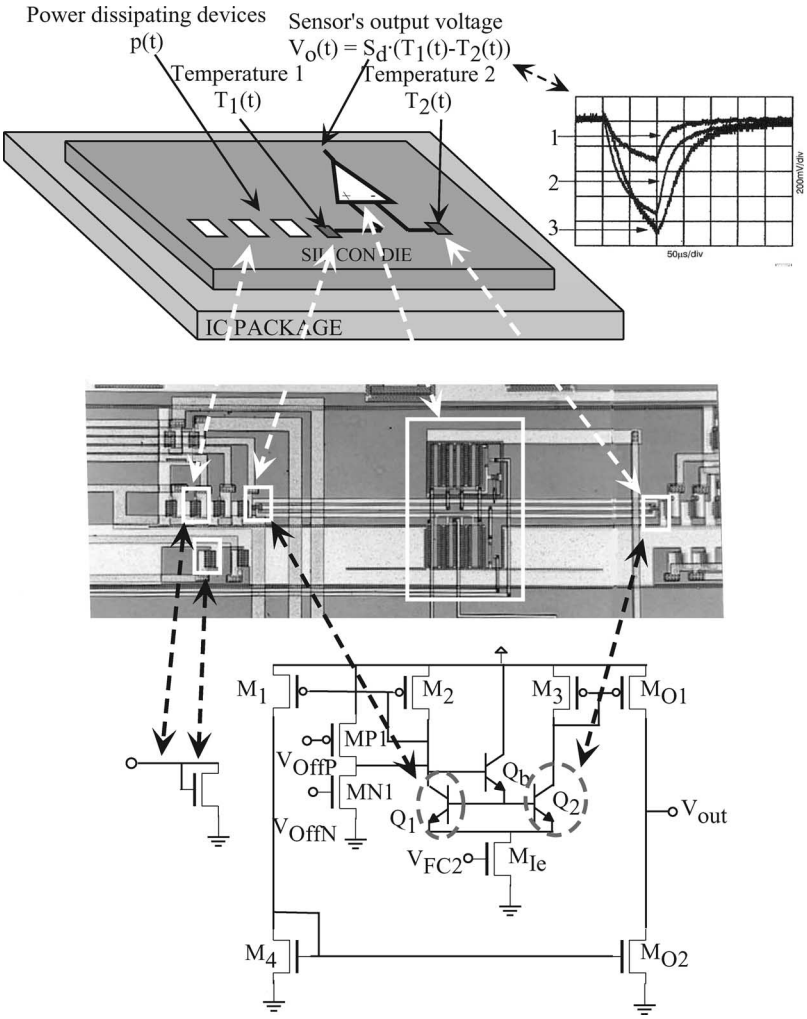

Fig. 13. ***Concept of differential temperature sensors and a BiCMOS realization. The figure shows the dynamic evolution of the implemented sensor when a device in the IC dissipates 23 mW during 100 μs.***

Nevertheless, lateral bipolar transistors have also been used for the design of CMOS temperature sensors. Examples can be found in [47].

Bipolar transistors display high dynamics. For instance, they have been used in [8] to characterize thermal couplings between devices of up to 100 kHz. In [48], a diode was used to record thermal transients up to 7 s with a sampling period of 400 μs to extract thermal impedances of packages in different mounting configurations.

MOS transistors have also been used as temperature sensitive devices. In an MOS transistor working in strong inversion, there are two parameters that are predominantly sensitive to temperature: the carrier's mobility μ and its threshold voltage Vt, from [49]

$$\mu(T) = \mu(T_0)\left(\frac{T}{T_0}\right)^{-k_1} \tag{4}$$

$$Vt(T) = Vt(T_0) - k_2(T - T_0). \tag{5}$$

Typical values for k_1 are between 1.5 and 2, whereas typical values for k_2 are between 0.5 mV/K and 4 mV/K. For instance, [50] suggests a value of $k_1 = 2$ for modern technologies, whereas [51] measures a value of $k_2 = 1.41$ mV/K for a 0.18-μm CMOS technology. In [52] $k_2 = 1.8$ mV/K is suggested for a 0.8-μm process. These parameters depend on the temperature. This dependence is studied in [50].

The main drawback of MOS transistors operating as temperature sensors is that their sensitivity depends on process-dependent parameters, such as threshold voltage, and not on physical constants, as is the case with the bipolar transistors. That makes this type of sensors process-dependent [52].

The effect of (4) and (5) over the drain current is for gate-source voltage biases close to the threshold voltage, the threshold voltage dominates the temperature dependence and the drain current has positive temperature coefficient. For gate-source voltage biases much higher

than the threshold voltage, the dependence on the temperature of the mobility dominates and the drain current has a negative temperature coefficient. In between both extreme biases, there is a gate source voltage for which the drain current has a null temperature coefficient [50].

If the MOS transistor works in weak inversion, the current follows the same diffusion process as in a bipolar transistor, and the temperature dependence has a similar expression.

There is a wide variety of multiple-device temperature sensors. For any sensor to be used as a thermal monitor, it should exhibit minimum area overhead and a simple structure. In this context, several works use a temperature-dependent digital oscillator, which provides digital readout in the form of temperature-dependent frequency. By way of example, in [50] a digital oscillator with an output frequency in the 1–3-MHz range, which decreases at a rate of −8 to −6 KHz/K depending on the bias voltage (from 5 to 2.5 V), is presented. In [17], it is suggested that ring oscillators are used to monitor the temperature in FPGAs. FPGAs allow dynamic reconfiguration of their hardware and, therefore, dynamic placement of temperature sensors. The implemented oscillators have an oscillating frequency between 21 and 27 MHz at 25 °C depending on the configuration, and the temperature sensitivity is $-0.20\%/^{\circ}\mathrm{C}$.

In [52], a sensor based on a threshold voltage reference is used as a thermal monitor. The advantage of this sensor is that the temperature dependence of both the mobility and the threshold voltage contribute in the same direction to the temperature dependence of the output current. Implemented in a 1-μm CMOS process, the main performances are as follows: area of 0.02 mm^2, power dissipation of 200 μW, temperature sensitivity of $-0.75\%/^{\circ}\mathrm{C}$, accuracy of ± 1 °C, and a sensitivity to power supply variations of $\pm 1\%$/V. The long-term stability was ± 0.5 °C over 160 days of continuous operation.

B. Differential Temperature Sensors

Differential temperature sensors are sensitive to the difference of temperature at two points of the silicon surface. Therefore, they provide immunity to any source that may introduce an offset to the thermal map at the silicon surface, e.g., variations in the ambient temperature. The use of differential temperature sensors has been reported in [53] as a part of a delayed short circuit protection in power ICs. In [19], its use has been proposed to detect dynamic thermal increases generated by undesired hot spots associated to defects in digital circuits, whereas in [54], their use has been suggested to measure the bandwidth of RF amplifiers through temperature measurements.

From an electrothermal point of view, differential temperature sensors are characterized by two parameters: their differential sensitivity, S_{dT}, and their common sensitivity, S_{cT}. The general expression for the output voltage of a differential sensor is

$$V_{\text{out}} = S_{dT}(T_2 - T_1) + S_{cT}\left(\frac{T_2 + T_1}{2}\right). \tag{6}$$

In order to obtain an effective differential temperature sensor, its differential sensitivity should be as high as possible, whereas its common sensitivity should ideally be zero. Similar to classical differential amplifiers, we can define a common mode rejection ratio (CMRR), defined as the ratio between the differential over the common sensitivity.

Focusing on possible realizations, they are categorized into passive and active.

Passive differential temperature sensors do not need a power supply and are based on the Seebeck effect that exists in thermocouples. The Seebeck effect is the difference of potential that exists at both ends of the conductor, V_{12}, due to a difference of temperature at these ends $(T_2 - T_1)$. The proportional factor between differences of voltage and temperature is called the Seebeck coefficient of the conductor α. As a matter of example, in [55] the Seebeck factor of the gate and capacitor polysilicons in a 1.2-μm CMOS technology were characterized with values of 105 and 96 μV/K, respectively. Other examples are reported in [65]. There, two thermocouples are placed at 5 μm from a dissipating device in a CMOS 0.35 technology. The thermopiles exhibit a differential sensitivity of 0.1 and 0.26 V per W dissipated by the device.

Active sensors need a source of energy. Compared with passive sensors, they exhibit a higher differential sensitivity with the drawback of the power consumption required to work. The general principle of an active differential sensor is the use of balanced circuits, for instance, current mirrors [56] or coupled-emitter (or source) stages [42], [53].

Temperature gradients in the circuit cause an unbalancing of the operating point.

Fig. 13 shows a schematic for a differential temperature sensor implemented in a 1.2-μm BiCMOS technology [6]. This sensor has been implemented in a test IC to dynamically track the power dissipated by devices placed in the same silicon IC. The circuit is based on a classic operational transconductance amplifier [66] (OTA). However, in this case, the differential input stage is not imbalanced by a different electrical biasing of the differential pair Q1 and Q2, but by a difference in its temperature. Therefore, to measure a temperature gradient, a distant placement of both devices is required. This is shown in the layout of the circuit: the distance between Q1 and Q2 is 500 μm. To compensate for thermal offsets due to mismatching between devices, the devices MN1 and MP1 have been added. For instance, with the bias of this

circuit being VFC2 = 1.7 V (@ VDD = 5 V), the differential sensitivity of the circuit is −2.7 V/°C.

To characterize the performances of the sensor, in the test IC some MOS transistors in diode configuration (i.e., source tied to GND and gate connected to the drain and to the bias voltage terminal [66]) have been placed (Fig. 13). The use of these MOS transistors is to dissipate power (and to change the IC surface thermal map) when they are driven by a voltage source. Thus, it is possible to observe the impact on the sensor's output caused by the static and dynamic activation of a specific device as a function of the distance between the dissipating device and the temperature sensitive device. Static measurements show that the sensor is very sensitive. For instance, the activation of an MOS transistor placed at 137 μm from Q1 and at 637 μm from Q2 gives a static sensitivity of −29.36 V per W dissipated at the MOS transistor. Fig. 13 shows the dynamic variation of the sensor's output voltage when an MOS transistor placed at 33 μm from Q1 and 533 μm from Q2 dissipates 23 mW during 100 μs. Three different plots are superimposed, corresponding to the three different biasing conditions of the sensor (Bias 1: $V_{FC2} = 1.95$, Bias 2: $V_{FC2} = 1.696$ V, Bias 3: $V_{FC2} = 1.2$ V), showing the dependence of the differential sensitivity and dynamic performances of the sensor on its biasing. In this figure, the vertical axis is 200 mV/div. As we can see, the use of differential temperature sensors provides a highly sensitive way to track power dissipated by devices and circuits.

If the distance between the temperature-sensitive devices of the sensor (Q1 and Q2) is long, we can assume that a small dissipation of power close to Q1 may not thermally affect Q2. In this case, differential temperature sensors can be used to characterize thermal couplings in ICs with high sensitivity. Fig. 2 is an example of the Bode diagrams of the thermal coupling in an IC measured with the differential sensor in Fig. 13.

VI. CONCLUSION

The dynamic evolution of the temperature on the surface of an IC is a projection of the circuit's behavior and IC structure. In this paper, we have focused on those measuring techniques that provide suitable performances for a reliable tracing of this dynamic, with detailed description of two measuring techniques: laser-based methods and embedded CMOS temperature sensors.

Temperature is a relevant physical variable for the design and the characterization of devices and circuits. The dynamics of the temperature contains information complementary to the traditional voltage and current electrical signals. The presented measuring techniques, along with their ongoing research, open new research scenarios for future generations of technology. ■

REFERENCES

[1] J. M. Soden and R. E. Anderson, "IC failure analysis: Techniques and tools for quality reliability improvement," *Proc. IEEE*, vol. 81, no. 5, pp. 703–715, May 1993.

[2] J. Hiatt, "A method of detecting hot spots on semiconductors using liquid crystals," in *Proc. 19th Annu. IEEE Reliability Physics Symp.*, 1981, pp. 130–133.

[3] D. H. Lee, "Thermal analysis of integrated circuit chips using thermographic imaging techniques," *IEEE Trans. Instrum. Meas.*, vol. 43, no. 6, pp. 824–829, Dec. 1994.

[4] P. Kolodner and J. A. Tyson, "Microscopic fluorescent imaging of surface temperature profiles with 0.01 °C resolution," *Appl. Phys. Lett.*, vol. 40, no. 9, pp. 782–784, 1982.

[5] J. Christofferson and A. Shakouri, "Thermal measurements of active semiconductor micro-structures acquired through the substrate using near IR thermoreflectance," *Microelectron. J.*, vol. 35, no. 10, pp. 791–796, Oct. 2004.

[6] J. Altet, A. Rubio, E. Schaub, S. Dilhaire, and W. Claeys, "Thermal coupling in integrated circuits: application to thermal testing," *IEEE J. Solid-State Circuits*, vol. 36, no. 1, pp. 81–91, Jan. 2001.

[7] D. J. Walkey, T. S. Smy, R. G. Dickson, J. S. Brodsky, D. T. Zweidinger, and R. M. Fox, "Equivalent circuit modeling of static substrate thermal coupling using VCVS representation," *IEEE J. Solid-State Circuits*, vol. 37, no. 9, pp. 1198–1205, Sep. 2002.

[8] N. Nenadovic, S. Mijalkovic, L. K. Nanver, L. K. J. Vandamme, V. d'Alessandro, H. Schellevis, and J. W. Slotboom, "Extraction and modeling of self-heating and mutual thermal coupling impedance of bipolar transistors," *IEEE J. Solid-State Circuits*, vol. 39, no. 10, pp. 1764–1772, Oct. 2004.

[9] F. F. Oettinger and D. L. Blackburn, "Semiconductor measurement technology: thermal resistance measurements, NIST Special Publication 400-86, Jul. 1990.

[10] T. S. Fisher, C. T. Avedisian, and J. P. Krusius, "Transient thermal response due to periodic heating on a convectively cooled substrate," *IEEE Trans. Compon., Packag., Manuf. Technol. B*, vol. 19, no. 1, pp. 255–261, Feb. 1996.

[11] M. Rencz and V. Székely, "Studies on the nonlinearity effects in dynamic compact model generation of packages," *IEEE Trans. Compon. Packag. Technol.*, vol. 27, no. 1, pp. 124–130, Mar. 2004.

[12] V. Székely and M. Renz, "Increasing the accuracy of thermal transient measurements," *IEEE Trans. Compon. Packag. Technol.*, vol. 25, no. 4, pp. 539–546, Dec. 2002.

[13] M. R. Rencz and V. Székely, "Measuring partial thermal resistance in a heat-flow path," *IEEE Trans. Compon. Packag. Technol.*, vol. 25, no. 4, pp. 547–553, Dec. 2002.

[14] K. Kurabayashi and K. E. Goodson, "Precision measurement and mapping of die-attach thermal resistance," *IEEE Trans. Compon., Packag., Manuf. Technol. A*, vol. 21, no. 3, pp. 506–514, Sep. 1998.

[15] M. Carmona, S. Marco, J. Palacín, and J. Samitier, "A time-domain method for the analysis of thermal impedance response preserving the convolution form," *IEEE Trans. Compon. Packag. Technol.*, vol. 22, no. 2, pp. 238–244, Jun. 1999.

[16] Pentium III processor active thermal management techniques (application note), Aug. 2000, order no. 273405-001.

[17] S. L. Buedo, J. Garrido, and E. I. Boemo, "Dynamically inserting, operating and eliminating thermal sensors on FPGA based systems," *IEEE Trans. Compon. Packag. Technol.*, vol. 26, no. 4, pp. 561–566, Dec. 2002.

[18] J. Altet and A. Rubio, *Thermal Testing of IC*. Norwell, MA: Kluwer, 2002.

[19] ——, "Differential sensing strategy for dynamic thermal testing of ICs," in *Proc. 15th IEEE VLSI Test Symp.*, 1997, pp. 434–439.

[20] D. Mateo, J. Altet, and E. Aldrete-Vidrio, "An approach to the electrical characterization of analog blocks through thermal measurements," in *Proc. 11th THERMINIC Workshop*, 2005, pp. 59–64.

[21] J. Christofferson and A. Shakouri, "Thermal measurements of active semiconductor micro-structures acquired through the substrate using near IR thermoreflectance," *Microelectron. J.*, vol. 35, no. 10, pp. 791–796, Oct. 2004.

[22] X. Perpinà, X. Jordà, N. Mestres, M. Vellvehi, P. Godignon, J. Millán, and H. von Kiedrowski, "Internal infrared laser deflection system: a tool for power device characterization," *Meas. Sci. Technol.*, vol. 15, no. 5, pp. 1011–1018.

[23] M. Nishiguchi, M. Fujihara, A. Miki, and H. Nishizawa, "Precision comparison of

surface temperaure measurement techniques for GaAs IC's," *IEEE Trans. Compon., Hybrids, Manuf. Technol.*, vol. 16, no. 5, pp. 543–549, Aug. 1993.

[24] W. Chen, H. Cheng, and H. Shen, "An effective methodology for thermal characterization of electronic packaging," *IEEE Trans. Compon., Hybrids, Manuf. Technol.*, vol. 26, no. 1, pp. 222–232, Mar. 2003.

[25] V. Székely and M. Rencz, "Image processing procedures for the thermal measurements," *IEEE Trans. Compon., Hybrids, Manuf. Technol.*, vol. 22, no. 2, pp. 259–265, Jun. 1999.

[26] J. Lai, M. Chandrachood, A. Majumdar, and J. P. Carrejo, "Thermal detection of device failure by atomic force microscopy," *IEEE Electron Device Lett.*, vol. 16, no. 7, pp. 312–315, Jul. 1995.

[27] J. Altet, J. M. Rampnoux, J. C. Batsale, S. Dilhaire, A. Rubio, W. Claeys, and S. Grauby, "Applications of temperature phase measurements to IC testing," *Microelectron. Reliab.*, vol. 44, pp. 95–103, 2004.

[28] S. Dilhaire, S. Grauby, W. Claeys, and J. C. Batsale, "Thermal parameters identification of micrometric layers of microelectronic devices by thermoreflectance," *Microsc. Microelectron. J.*, vol. 35, no. 10, pp. 811–816, Oct. 2004.

[29] L. D. Patiño Lopez, S. Grauby, S. Dilhaire, M. A. Salhi, W. Claeys, S. Lefèvre, and S. Volz, "Characterization of the thermal behavior of PN thermoelectric couples by scanning thermal microscope," *Microelectron. J.*, vol. 35, no. 10, pp. 797–803, Oct. 2004.

[30] W. Claeys, S. Dilhaire, V. Quintard, and Y. Danto, "Thermoreflectance optical test probe for the measurement of current induced temperature changes in microelectronic components," *Qual. Reliab. Eng. Int.*, vol. 9, pp. 303–308, 1993.

[31] W. Claeys, S. Dilhaire, and V. Quintard, "Laser probing of thermal behaviour of electronic components and its application in quality and reliability testing," *Microelectron. Eng.*, vol. 24, pp. 411–420, 1994.

[32] W. Claeys, S. Dilhaire, V. Quintard, J. P. Dom, and Y. Danto, "Thermoreflectance optical test probe for the measurement of current induced temperature changes in microelectronic components," *Qual. Reliab. Eng. Int.*, vol. 9, pp. 303–308, 1993.

[33] V. Quintard, G. Deboy, S. Dilhaire, D. Lewis, T. Phan, and W. Claeys, "Laser beam thermography of circuits in the particular case of passivated semiconductors," *Microelectron. Eng.*, vol. 31, pp. 291–298, 1996.

[34] S. Grauby, S. Dilhaire, S. Jorez, and W. Claeys, "Imaging setup for temperature, topography, and surface displacement measurements of microelectronic devices," *Rev. Sci. Instrum.*, vol. 74, no. 1, pp. 645–647, Jan. 2003.

[35] W. Claeys, S. Dilhaire, S. Jorez, and L.-D. Patino-Lopez, "Laser probes for the thermal and thermomechanical characterisation of microelectronic devices," *Microelectron. J.*, vol. 32, no. 10–11, pp. 891–898, Oct.–Nov. 2001.

[36] A. Rosencwaig, J. Opsal, N. L. Smith, and D. L. Willenborg, "Detection of thermal waves through optical reflectance," *Appl. Phys. Lett.*, vol. 46, pp. 1013, 1985.

[37] H. A. Weakliem and D. Redfield, "Temperature dependence of the optical properties of silicon," *J. Appl. Phys.*, vol. 50, no. 3, pp. 1491, 1979.

[38] S. Dilhaire, S. Jorez, L. D. Patiño-Lopez, W. Claeys, and E. Schaub, "Calibration procedure of temperature measurements by thermoreflectance upon microelectronic devices." presented at the 11th Int. Conf. Photoacoustic and Photothermal Phenomena, Kyoto, Japan, 2000.

[39] S. Dilhaire, E. Schaub, W. Claeys, J. Altet, and A. Rubio, "Localisation of heat sources in electronicrcuits by microthermal laser probing," *Int. J. Therm. Sci.*, vol. 39, pp. 544–549, 2000.

[40] S. Dilhaire, J. Altet, S. Jorez, E. Schaub, A. Rubio, and W. Claeys, "Fault localisation in IC's by goniometric laser probing of thermal induced surface waves," *Microelectron. Reliab.*, vol. 39, pp. 919–923, 1999.

[41] J. Altet, M. A. Salhi, S. Dilhaire, and A. Ivanov, "Calibration-free heat source localization in ICs entirely covered by metal layers," *Electron. Lett.*, vol. 40, no. 4, pp. 241–242, Feb. 19, 2004.

[42] J. Altet, A. Rubio, A. Salhi, J. L. Galvez, S. Dilhaire, A. Syal, and A. Ivanov, "Sensing temperature in CMOS circuits for thermal testing," in *Proc. 22nd IEEE VLSI Test Symp.*, 2004, pp. 179–184.

[43] S. Dilhaire, S. Grauby, S. Jorez, L. D. P. Lopez, J.-M. Rampnoux, and W. Claeys, "Surface displacement imaging by interferometry with a light emitting diode," *Appl. Opt.*, vol. 41, no. 24, pp. 4996–5001, Aug. 20, 2002.

[44] V. Székely, C. Márta, M. Rencz, Z. Benedek, and B. Courtois, "Design for thermal testability (DfTT) and a CMOS realization," *Sens. Actuators*, vol. A55, no. 1, pp. 29–34, 1996.

[45] G. C. M. Meijer, G. Wang, and F. Fruett, "Temperature sensors and voltage references implemented in CMOS technology," *IEEE Sensors J.*, vol. 1, no. 3, pp. 225–234, Oct. 2001.

[46] A. Bakker and J. H. Huijsing, "Micropower CMOS temperature sensor with digital output," *IEEE J. Solid-State Circuits*, vol. 31, no. 7, pp. 933–937, Jul. 1996.

[47] R. A. Bianchi, J. M. Karam, B. Courtois, R. Nadal, F. Pressecq, and S. Sifflet, "CMOS-compatible temperature sensor with digital output for wide temperature range applications," *Microelectron. J.*, vol. 31, no. 9–10, pp. 803–810, Oct. 2000.

[48] P. E. Bagnoli, C. Casarosa, E. Dallago, and M. Nardoni, "Thermal resistance analysis by induced transient (TRAIT) method for power electronic devices thermal characterization—Part II: Practice and experiments," *IEEE Trans. Power Electron.*, vol. 13, no. 6, pp. 1220–1228, Nov. 1998.

[49] Y. P. Tsividis, *Operation and Modeling of the MOS Transistor*. New York: McGraw-Hill, 1987.

[50] I. M. Filanovsky and A. Allan, "Mutual compensation of mobility and threshold voltage temperature effects with application in CMOS circuits," *IEEE Trans. Circuits Syst. I, Fundam. Theory Appl.*, vol. 48, no. 7, pp. 876–884, Jul. 2001.

[51] I. M. Filanovsky and S. T. Lim, "Temperature sensor applications of diode-connected MOS transistors," in *IEEE Int. Symp. Circuits and Systems*, 2002, pp. II-149–II-152.

[52] V. Székely, C. Marta, Z. Kohari, and M. Rencz, "CMOS sensors for on-line thermal monitoring of VLSI circuits," *IEEE Trans. Very Large Scale Integr. (VLSI) Syst.*, vol. 5, no. 3, pp. 270–276, Sep. 1997.

[53] P. Antognetti, G. R. Bisio, F. Curatelli, and S. Palara, "Three-dimensional transient thermal simulation: Application to delayed short circuit protection in power ICs," *IEEE J. Solid-State Circuits*, vol. SC-15, no. 3, pp. 277–281, Jun. 1980.

[54] J. Altet, D. Mateo, and J. L. Gonzalez, "Observation of high-frequency analog/RF electrical circuit characteristics by on-chip thermal measures," in *Proc. ISCAS 2006*.

[55] M. V. Arx, O. Paul, and H. Baltes, "Test structures to measure the Seebeck coefficient of CMOS IC polysilicon," *IEEE Trans. Semicond. Manuf.*, vol. 10, no. 2, pp. 201–208, May 1997.

[56] A. Syal, V. Lee, A. Ivanov, and J. Altet, "CMOS differential and absolute thermal sensor," *J. Electron. Testing: Theory Appl.*, vol. 18, pp. 295–304, 2002.

[57] O. Breitenstein, M. Langenkamp, F. Altmann, D. Katzer, A. Lindner, and H. Eggers, "Microscopic lock-in thermography investigation of leakage sites in integrated circuits," *Rev. Sci. Instrum.*, vol. 7, no. 11, pp. 4155–4160, Nov. 2000.

[58] K. Arabi and B. Kaminska, "Built-in temperature and current sensors for on-line oscillation-testing," in *Proc. 2nd IEEE Int. On-Line Testing Workshop*, 1996, pp. 13–16.

[59] D. L. Blackburn, "Temperature measurements of semiconductor devices—A review," in *Proc. 20th SEMITHERM Symp.*, 2004, pp. 70–80.

[60] S. Volz, S. Dilhaire, S. Lefebvre, and L. D. Patino-Lopez, Scanning thermal microscopy applied to thin films and electronic devices characterization," *Handbook of Semiconductor Nanostructures and Nanodevices*, A. A. Balandin and K. L. Wang, Eds. North Lewis Way, CA: American Scientific, ch. 29.

[61] I. Abbadi, "New imaging method for diffusive and opaque media: Application to backside imaging of integrated circuits," Ph.D. dissertation, Univ. Bordeaux 1, Bordeaux, France, 2005.

[62] J. Altet, S. Dilhaire, S. Volz, J. M. Rampnoux, A. Rubio, S. Grauby, L. D. Patino-López, W. Claeys, and J. B. Saulnier, "Four different approaches for the measurement of IC surface temperature: Application to thermal testing," *Microelectron. J.*, vol. 33, pp. 689–696, 2002.

[63] J. Altet, M. A. Salhi, S. Dilhaire, A. Syal, and A. Ivanov, "Localisation of devices acting as heat sources in ICs covered enterely by metal layers," *Electron. Lett.*, vol. 39, no. 20, pp. 1140–1442, 2003.

[64] H. S. Carslaw and J. C. Jaeger, *Conduction Heat in Solids*. New York: Oxford, 1993.

[65] E. Aldrete, J. Altet, and D. Mateo, "Differential temperature sensors in 0.35 μm CMOS technology," in *Proc. IEEE THERMINIC 2005 Conf.*, pp. 122–128.

[66] K. R. Laker and W. Sansen, *Design of Analog Integrated Circuits and Systems*. New York: Mc Graw-Hill, 1994.

[67] P. Jeong, W. S. Moo, and C. C. Lee, "Thermal modeling and measurement of GaN-based HFET devices," *IEEE Electron Device Lett.*, vol. 24, no. 7, pp. 424–426, Jul. 2003.

[68] A. M. Chaudhari, T. M. Woudenberg, M. Albin, and K. E. Goodson, "Transient liquid crystal thermometry of microfabricated PCR vessel arrays," *J. Microelectromech. Syst.*, vol. 7, no. 4, pp. 345–355, 1998.

ABOUT THE AUTHORS

Josep Altet received the Technical Telecommunication Engineering and the Electronic Engineering degrees from the Ramon Llull University, (URL) Barcelona, Spain, and the Ph.D. degree from the Technical University of Catalonia (UPC), Barcelona.

He is now an Associate Professor in the Department of Electronic Engineering, UPC. His research interests include VLSI design and test, temperature sensor design, and thermal coupling analysis and modeling in integrated circuits.

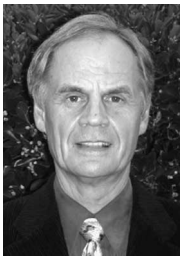

Wilfrid Claeys received the Ph.D. degree in 1974 at the University of Louvain, Louvain, Belgium.

He was an Assistant Professor at the University of Louvain. He has been a Professor at the University of Bordeaux, Bordeaux, France, since 1990. He is leading a research group dedicated to optical probing of the thermal behavior of microelectronics components.

Stefan Dilhaire received both an undergraduate degree in microelectronics and the Ph.D. degree in electronics from the University of Bordeaux, Bordeaux, France.

He is now an associate professor at the University of Bordeaux. His work involves the design of optical contactless probes for analyzing the thermal behavior of integrated circuits.

Antonio Rubio received the M.S. and Ph.D. degrees from the Industrial Engineering Faculty of Barcelona, Spain.

He has been Associate Professor of the Electronic Engineering Department at the Industrial Engineering Faculty, Technical University of Catalonia (UPC), Barcelona, and Professor of the Physics Department at the Balearic Islands University. He is currently Professor of Electronic Technology at the Telecommunication Engineering Faculty, UPC. His research interests include very large scale integration (VLSI) design and test, device and circuit modeling and high-speed circuit design.